

The connection between shear and star formation in spiral galaxies

Marc S. Seigar^{*}

Department of Physics & Astronomy, University of California Irvine, 4129 Frederick Reines Hall, Irvine, CA 92697-4575, USA

Accepted 2005 April 24. Received 2005 April 22; in original form 2005 March 30.

ABSTRACT

We present a sample of 33 galaxies for which we have calculated (i) the average rate of shear from published rotation curves, (ii) the far-infrared luminosity from IRAS fluxes and (iii) the K-band luminosity from 2MASS. We show that a correlation exists between the shear rate and the ratio of the far-infrared to K-band luminosity. This ratio is essentially a measure of the star formation rate per unit mass, or the specific star formation rate. From this correlation we show that a critical shear rate exists, above which star formation would turn off in the disks of spiral galaxies. Using the correlation between shear rate and spiral arm pitch angle, this shear rate corresponds to the lowest pitch angles typically measured in near-infrared images of spiral galaxies.

Key words: galaxies: fundamental parameters – galaxies: spiral – infrared: galaxies

1 INTRODUCTION

Jeans (1929) took up the question of self-gravitating gas and found that under certain conditions it could be unstable enough to collapse under its own self-gravity. In order to show this he considered an adiabatic gas. A similar calculation can be applied to stellar systems.

The idea of instabilities is essentially a condensation of material, so in order for material to condense it is necessary to find out if gravity will cause collapse before velocity dispersion causes expansion. A characteristic time can be calculated for each process and compared to see which process is dominant. It turns out that on small scales velocity dispersion is dominant, and on large scales gravity is dominant. Jeans (1929) found a critical length above which gravitational instability becomes dominant, now known as the Jeans length, L_{Jeans} .

The situation in the disks of galaxies is different from the problem formulated by Jeans, due to the flatness of the system (instead of a spheroid assumed in the Jeans analysis) and more importantly, differential rotation. Velocities due to differential rotation are approximately proportional to ΔR and might even prevent the collapse from taking place, even at distances greater than the Jeans length. Differential rotation inhibits the gravitational collapse on large scales. The question is what happens in between? Toomre (1964) attempted to answer this question. He investigated the balance between differential rotation and self-gravitation. Differential rotation manifests itself physically from the fact that a contracting region conserves angular momentum. This spins

up and causes a centrifugal force that might inhibit further collapse. Toomre (1964) found that differential rotation implies that disks are stabilised at lengths greater than a critical length, which we will call the rotation length, L_{rot} . It turns out that L_{rot} is inversely proportional to the average angular velocity with respect to a fixed system. The higher the average angular velocity, the greater the rate of shear, A/ω . In other words as the rate of shear increases, the value of L_{rot} decreases, until it reaches the limiting case where $L_{rot} = L_{Jeans}$, and the entire disk is stable against gravitational collapse, i.e. no clouds will collapse and therefore no star formation can occur.

In reality most disks have a region where they are unstable to gravitational instabilities and this region has a length scale between the Jeans length and the rotation length, i.e. $L_{Jeans} < L < L_{rot}$. However, the faster a disk rotates, the stronger its differential rotation. The stronger differential rotation becomes, the more inhibited star formation becomes, and thus we expect a correlation between star formation rate and shear rate.

Toomre (1964) derived a value of the velocity dispersion for the limiting regime where $L_{rot} = L_{Jeans}$, i.e. a critical velocity dispersion. The stability of disks can then be quoted as the ratio of the actual velocity dispersion to the critical velocity dispersion, Q . Thus if $Q > 1$ then the velocity dispersion is high enough to prevent gravitational collapse, and if $Q < 1$ then gravitational collapse occurs. This condition is known as the *Toomre stability criterion* and the parameter Q is known as *Toomre's parameter*.

Since differential rotation acts to shear features in the disk, the shear rate is a viable quantity for measuring the differential rotation in the disks of spiral galaxies. Shear rate

^{*} E-mail: mseigar@uci.edu

has been measured by several authors (e.g. Block et al. 1999; Seigar, Block & Puerari 2004; Seigar et al. 2005) and can be measured directly from a galaxy rotation curve. The sequence of low shear rates to high shear rates also follows the sequence from late-type spirals to early-type spirals (Seigar et al. 2005). It has been shown that as one progresses along the Hubble sequence, the specific star formation rate (measured as the H α equivalent width) in galaxies increases (e.g. James et al. 2004). If one takes this along with the correlation between pitch angle and shear rate in Seigar et al. (2005), then the existence of a correlation between shear rate and specific star formation rate is implied, assuming that the transition from tightly wound spiral structure to loosely wound spiral structure follows the Hubble sequence from early- to late-type spiral galaxies.

This letter is arranged as follows. Section 2 describes the data we have used. Section 3 describes how shear rates were calculated using rotation curves. Section 4 describes a method for determining the star formation rate per unit surface area. Finally, section 5 discusses the results.

2 DATA

In order to calculate shear rates, rotation curves are required. Burstein & Rubin (1985) presented data for 60 galaxies for which they had observed rotation curves. The rotation curve data was available in a series of papers from the early 1980s (Rubin, Ford & Thonnard 1980; Rubin et al. 1982, 1985). Of this sample of 60 galaxies, 40 were detected by IRAS at 60 μ m and 100 μ m, and by 2MASS in the K_s -band. 6 of these galaxies were rejected from our sample, as they were classified as HII or starburst and may therefore have external physical processes affecting their star formation rates. A further object did not have a rotation curve that covered a sufficient radial range and was also not included in the sample. The remaining 33 galaxies are presented here.

3 CALCULATION OF SHEAR RATE

The rotation curves presented by Rubin et al. (1980, 1982, 1985) are of good quality and can be used to derive shear rates. The rates of shear are derived from their rotation curves as follows,

$$\frac{A}{\omega} = \frac{1}{2} \left(1 - \frac{R}{V} \frac{dV}{dR} \right) \quad (1)$$

where A is the first Oort constant, ω is the angular velocity and V is the measured line-of-sight velocity at a radius R . The value of A/ω is the shear rate.

Using equation (1), we have calculated mean shear rates for these galaxies, over a radial range with the inner limit near the turnover radius, and the outer limit at the D_{25} radius. The dominant source of error on the shear rate is the spectroscopic errors (i.e. a combination of the intrinsic spectroscopic error and the error associated with folding the two sides of the galaxy), which Rubin et al. (1980, 1982, 1985) claim is quite small, typically < 10 per cent. In order to calculate the shear rate, the mean value of dV/dR measured in km s $^{-1}$ arcsec $^{-1}$ is calculated by fitting a line of constant gradient to the outer part of the rotation curve (i.e. past the radius of rotation). This results in a mean shear rate.

This is essentially the same method used by other authors to calculate shear rate (e.g. Block et al. 1999; Seigar, Block & Puerari 2004; Seigar et al. 2005). The shear rates for these galaxies are listed in Table 1.

4 IRAS FLUXES AS AN INDICATOR OF STAR FORMATION RATES

The IRAS 60 μ m and 100 μ m fluxes have been used to calculate the far-infrared luminosity for the galaxies in this sample for which IRAS data was available (see Table 1). The far-infrared luminosity L_{FIR} can be used as a quantitative indicator of star formation rates (Spinoglio et al. 1995; Seigar & James 1998a). This was divided by the K-band luminosity L_K of the galaxies to compensate for differences in their overall size. The K band luminosity can be used to estimate the stellar mass in galaxies (e.g. Brinchmann & Ellis 2000; Gavazzi et al. 2002) and so the L_{FIR}/L_K ratio can be interpreted as a star formation rate per unit stellar mass, i.e. a specific star formation rate. This is closely related to the birthrate parameter (Gavazzi et al. 2002), i.e. the fraction of young to old stars. The far-infrared luminosity in terms of the 60 μ m and 100 μ m flux is given by Lonsdale et al. (1985) as,

$$L_{FIR} = 3.75 \times 10^5 D^2 (2.58S_{60} + S_{100}) \quad (2)$$

where L_{FIR} is the far-infrared luminosity in solar units, D is the distance to the galaxy in Mpc, S_{60} is the 60 μ m flux in Jy and S_{100} is the 100 μ m flux in Jy. As these galaxies are nearby, for the calculation of distance D , a simple Hubble flow is assumed and a Hubble constant, $H_0 = 75$ km s $^{-1}$ Mpc $^{-1}$, is adopted.

Given an apparent K-band magnitude it is possible to calculate a K-band luminosity using a relationship from Seigar & James (1998a),

$$\log_{10} L_K = 11.364 - 0.4K_T + \log_{10} (1 + z) + 2 \log_{10} D \quad (3)$$

where L_K is the K-band luminosity in solar units, K_T is the K-band apparent magnitude and z is the redshift of the galaxy. The $\log_{10} (1 + z)$ term is a first order K-correction. In order to calculate this total K-band luminosity, apparent K-band magnitudes from the 2MASS survey were used.

5 DISCUSSION

Fig. 1 shows a plot of the ratio of far-infrared luminosity to K-band luminosity versus shear rate. A good correlation is shown (correlation coefficient = 0.71; significance = 99.91%). This is essentially a correlation between the star formation rate per unit stellar mass (or the specific star formation rate) and shear rate. This correlation has been used to determine the relationship between shear rate and the far-infrared luminosity as follows,

$$\frac{L_{FIR}}{L_K} = (0.269 \pm 0.020) - (0.386 \pm 0.040) \left(\frac{A}{\omega} \right) \quad (4)$$

Where L_{FIR} is the far-infrared luminosity, L_K is the K-band luminosity and A/ω is the shear rate. The relationship between star formation rate (in M_\odot /year) and the far-infrared luminosity (in ergs/s) for normal spiral galaxies is given by Buat & Xu (1996) as

Table 1. Data for the 33 galaxies. Column 1 lists the name of the galaxy; Column 2 lists the Hubble type from de Vaucouleurs et al. (1991; hereafter RC3); Column 3 lists the shear rates as calculated from the rotation curves; Column 4 lists the IRAS 60 μ m flux; Column 5 lists the IRAS 100 μ m flux; Column 6 lists the distance to the objects in Mpc; Column 7 lists the diameters out to the $\mu_R = 25$ mag arcsec $^{-2}$ isophote (D_{25}) from RC3; Column 8 lists the far-infrared luminosity in solar units calculated using equation 2; Column 9 lists the apparent K $_s$ -band total magnitude from 2MASS; Column 10 lists the K-band luminosity calculated using equation 3 and column 11 lists the inferred star formation rate.

Galaxy name	Hubble Type	Shear rate	S_{60} (Jy)	S_{100} (Jy)	D (Mpc)	D_{25} (kpc)	L_{FIR} ($\times 10^9 L_{\odot}$)	K_T	L_K ($\times 10^{10} L_{\odot}$)	SFR ($M_{\odot}/year$)
NGC 753	SABbc	0.38 \pm 0.03	3.36	11.40	65.4	47.79 \pm 2.25	32.17 \pm 2.25	9.37 \pm 0.02	17.88 \pm 0.33	8.30 \pm 1.71
NGC 801	Sc	0.53 \pm 0.03	1.45	5.06	76.9	70.73 \pm 5.05	19.47 \pm 1.27	9.51 \pm 0.03	21.82 \pm 0.59	6.20 \pm 1.19
NGC 1024	SAab	0.65 \pm 0.02	0.57	2.62	47.1	53.30 \pm 2.54	3.40 \pm 0.49	8.74 \pm 0.02	16.49 \pm 0.30	2.31 \pm 0.43
NGC 1035	SAC?	0.37 \pm 0.03	3.57	11.12	16.6	10.81 \pm 0.77	2.09 \pm 0.13	9.13 \pm 0.01	1.42 \pm 0.01	0.68 \pm 0.14
NGC 1085	SAbc	0.52 \pm 0.04	0.88	3.16	90.5	77.69 \pm 7.50	16.71 \pm 1.25	9.80 \pm 0.03	23.40 \pm 0.64	6.90 \pm 1.40
NGC 1357	SAab	0.56 \pm 0.03	0.93	4.67	26.8	21.97 \pm 1.57	1.90 \pm 0.21	8.42 \pm 0.03	7.18 \pm 0.20	1.78 \pm 0.34
NGC 1417	SABb	0.45 \pm 0.03	1.59	5.82	54.2	42.43 \pm 3.03	10.95 \pm 0.60	9.14 \pm 0.03	15.28 \pm 0.42	5.81 \pm 1.15
NGC 1421	SABbc	0.31 \pm 0.04	8.48	21.32	27.8	28.69 \pm 1.35	12.55 \pm 0.69	8.40 \pm 0.02	7.91 \pm 0.14	4.34 \pm 1.05
NGC 1620	SABbc	0.44 \pm 0.03	1.31	5.31	46.8	39.26 \pm 2.80	7.15 \pm 0.43	8.92 \pm 0.03	13.91 \pm 0.38	5.46 \pm 1.08
NGC 2590	SAbc	0.44 \pm 0.03	2.01	6.03	66.6	43.38 \pm 3.08	18.68 \pm 0.93	9.38 \pm 0.03	18.43 \pm 0.50	7.24 \pm 1.44
NGC 2608	SBb	0.45 \pm 0.04	2.25	5.77	28.5	18.99 \pm 0.90	3.51 \pm 0.23	9.33 \pm 0.03	3.51 \pm 0.10	1.33 \pm 0.28
NGC 2639	SAa?	0.54 \pm 0.03	1.99	7.06	44.5	23.56 \pm 2.87	9.04 \pm 0.36	8.40 \pm 0.03	20.25 \pm 0.55	5.51 \pm 1.07
NGC 2742	SAC	0.40 \pm 0.03	3.08	10.49	17.2	15.11 \pm 1.08	2.04 \pm 0.10	8.81 \pm 0.01	2.06 \pm 0.02	0.91 \pm 0.18
NGC 2775	SAab	0.63 \pm 0.03	1.80	9.46	18.1	22.46 \pm 1.06	1.74 \pm 0.12	7.04 \pm 0.02	11.60 \pm 0.21	1.90 \pm 0.36
NGC 2815	SBb	0.60 \pm 0.03	1.04	4.79	33.9	34.19 \pm 1.03	3.21 \pm 0.27	8.25 \pm 0.03	13.44 \pm 0.37	2.68 \pm 0.52
NGC 2844	SAa	0.63 \pm 0.03	0.41	1.91	19.8	8.92 \pm 0.64	0.44 \pm 0.06	9.89 \pm 0.03	1.01 \pm 0.03	0.16 \pm 0.04
NGC 2998	SABc	0.41 \pm 0.03	1.58	4.63	63.8	53.53 \pm 2.52	13.28 \pm 0.93	9.93 \pm 0.04	10.23 \pm 0.37	4.39 \pm 0.89
NGC 3223	SAbc	0.61 \pm 0.03	3.79	14.76	38.6	45.75 \pm 2.16	13.71 \pm 1.51	7.58 \pm 0.02	32.22 \pm 0.59	6.06 \pm 1.16
NGC 3281	SABa	0.45 \pm 0.02	6.86	7.51	42.7	41.13 \pm 2.94	17.21 \pm 1.20	8.31 \pm 0.03	20.19 \pm 0.55	7.68 \pm 1.44
NGC 3495	Sd	0.42 \pm 0.02	1.82	7.28	15.2	21.66 \pm 1.02	1.03 \pm 0.08	8.93 \pm 0.02	1.43 \pm 0.03	0.60 \pm 0.11
NGC 3672	SAC	0.43 \pm 0.02	7.33	20.80	24.8	30.08 \pm 1.42	9.18 \pm 0.78	8.27 \pm 0.01	7.08 \pm 0.06	2.86 \pm 0.53
NGC 4378	SAa	0.69 \pm 0.03	0.36	1.45	34.1	28.61 \pm 1.35	1.04 \pm 0.18	8.51 \pm 0.02	10.71 \pm 0.20	1.00 \pm 0.18
NGC 4682	SABcd	0.51 \pm 0.03	0.69	2.38	31.1	23.25 \pm 1.66	1.51 \pm 0.14	9.60 \pm 0.02	3.25 \pm 0.06	1.00 \pm 0.20
NGC 6314	SAa	0.60 \pm 0.03	0.51	2.85	88.4	37.16 \pm 3.60	12.18 \pm 1.10	9.81 \pm 0.03	22.12 \pm 0.60	4.43 \pm 0.84
NGC 7083	SABc	0.43 \pm 0.03	5.02	17.19	41.5	49.96 \pm 2.36	19.41 \pm 0.87	8.42 \pm 0.03	17.17 \pm 0.47	6.95 \pm 1.39
NGC 7171	SBb	0.47 \pm 0.03	0.89	3.33	36.3	27.77 \pm 1.31	2.77 \pm 0.18	9.31 \pm 0.04	5.78 \pm 0.21	2.06 \pm 0.41
NGC 7217	SAab	0.66 \pm 0.02	4.96	18.45	12.7	14.37 \pm 0.68	1.89 \pm 0.17	6.83 \pm 0.01	6.93 \pm 0.06	0.89 \pm 0.16
IC 467	SABc	0.50 \pm 0.04	0.89	3.16	27.2	25.60 \pm 1.21	1.52 \pm 0.10	10.04 \pm 0.05	1.66 \pm 0.07	0.53 \pm 0.11
IC 724	Sa	0.69 \pm 0.03	0.34	1.27	79.6	54.28 \pm 5.23	5.09 \pm 0.81	9.39 \pm 0.04	26.10 \pm 0.94	2.40 \pm 0.44
UGC 3691	SACd	0.33 \pm 0.03	1.36	3.79	29.4	18.71 \pm 1.80	2.36 \pm 0.21	10.31 \pm 0.07	1.51 \pm 0.09	0.80 \pm 0.16
UGC 10205	Sa	0.48 \pm 0.03	0.39	1.54	87.4	36.74 \pm 4.50	7.32 \pm 1.02	9.89 \pm 0.03	19.98 \pm 0.54	6.88 \pm 1.35
UGC 11810	SABbc	0.42 \pm 0.02	0.50	2.04	63.0	33.35 \pm 1.57	4.93 \pm 0.57	10.82 \pm 0.06	4.38 \pm 0.24	1.81 \pm 0.34
UGC 12810	SABbc	0.44 \pm 0.02	0.78	1.78	108.2	58.61 \pm 5.63	16.59 \pm 1.99	10.47 \pm 0.06	18.04 \pm 0.97	7.08 \pm 1.33

$$SFR(M_{\odot}/year) = 8 \times 10^{-44} L_{FIR}(ergs/s) \quad (5)$$

This has been used to calculate the star formation rates listed in Table 1.

Galaxies with higher shear rates have tighter spiral structure. These are the early-type galaxies (Seigar, Block & Puerari 2004; Seigar et al. 2005). Those with low shear rates have loosely wound spiral structure. These are the late-type galaxies. The transition from early-type to late-type spiral galaxies also follows a transition from galaxies with low amounts of gas to gas-rich galaxies (Bertin 1991; Block et al. 1994; Bertin & Lin 1996). Therefore later-type spirals have more gas with which to form stars and it therefore follows that late-type spiral galaxies might have larger specific star-formation rates than early-type spiral galaxies. Such a correlation has been shown and discussed by James et al. (2004), who show that a correlation exists between H α equivalent width (which is related to the specific star formation rate and the birthrate parameter) and galaxy type. Is it therefore possible that the correlation shown in Fig. 1 is affected by a selection bias such as the one described here?

In an attempt to answer this we have investigated the relationship between shear rate and morphological type (Fig. 2), and L_{FIR}/L_K and morphological type (Fig. 3). Fig. 2 shows a weak and insignificant correlation (correlation coefficient=0.24; significance=70.90 per cent). Although it is insignificant the correlation is in the expected sense, with early type galaxies have higher rates of shear. The weakness of the correlation may be attributed to the problems associated with assigning galaxies with a Hubble type, which is usually a process that is done by eye and sometimes bears little resemblance to the underlying stellar mass distribution (Seigar & James 1998a, b; Seigar et al. 2005). Fig. 3 also shows a weak and insignificant correlation (correlation coefficient=0.20; significance=83.29 per cent), although once again the correlation is in the expected sense. Given the weakness, and the low significance of the correlations shown in Fig. 2 and Fig. 3, it is unlikely that the good correlation between shear rate and L_{FIR}/L_K is a selection affect.

We believe that the correlation shown in Fig. 1 is a useful diagnostic tool. Given a rotation curve and far-infrared

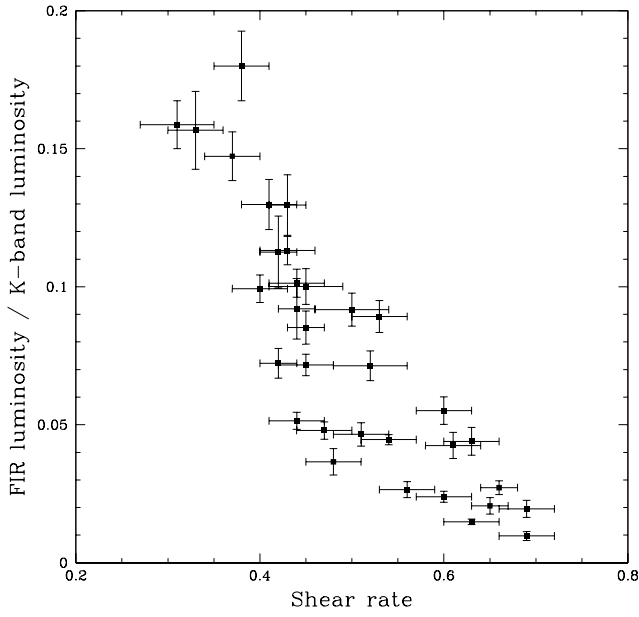


Figure 1. Shear rate, A/ω , versus ratio of FIR to K-band luminosity, L_{FIR}/L_K

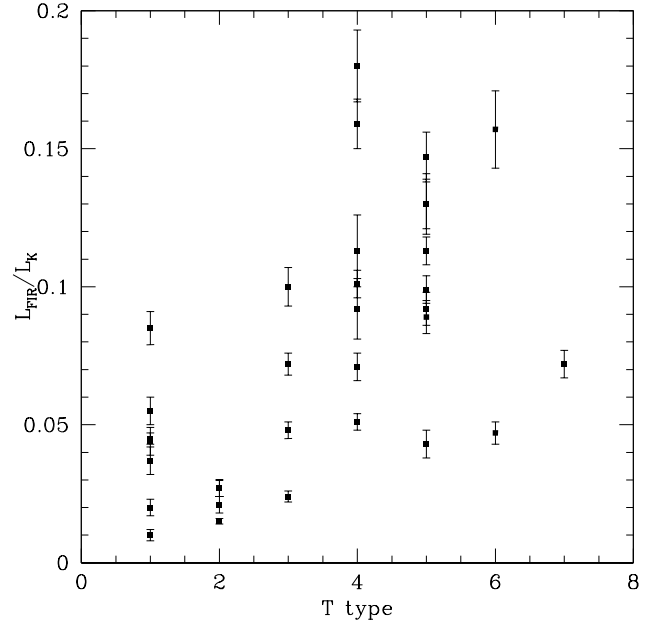


Figure 3. T type versus ratio of FIR to K-band luminosity, L_{FIR}/L_K

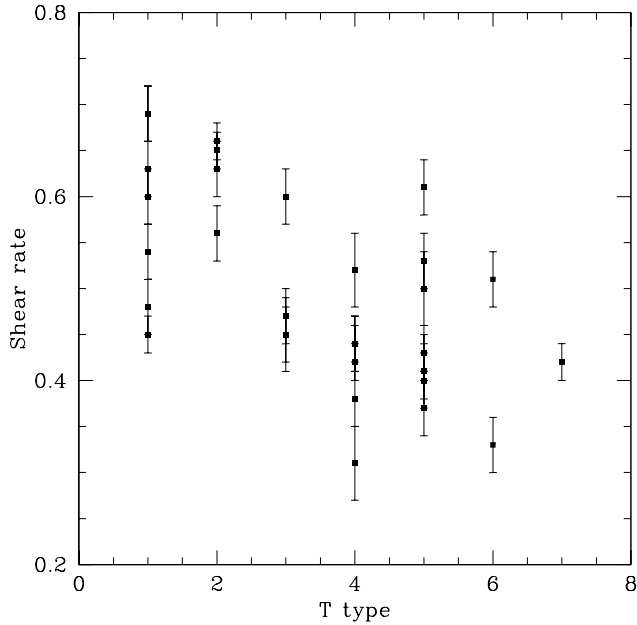


Figure 2. T type versus shear rate

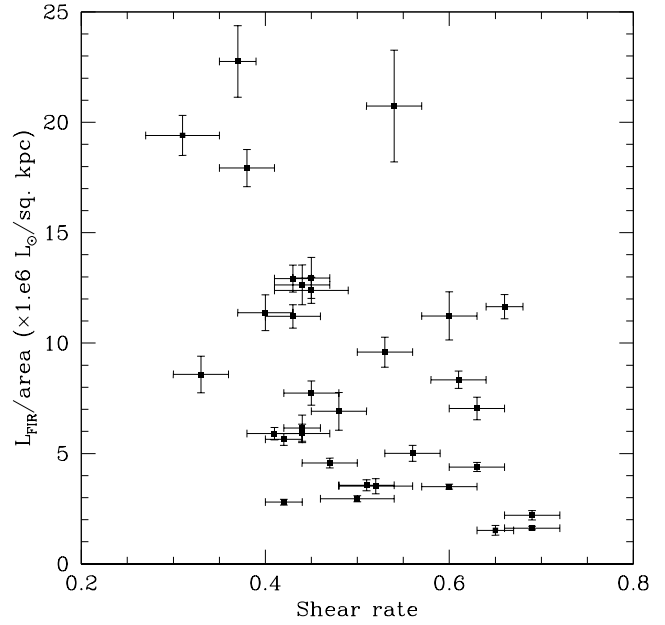


Figure 4. Shear rate, A/ω , versus star formation rate per unit area in $M_\odot \text{ year}^{-1} \text{ kpc}^{-2}$.

data for a galaxy, it should be possible to measure the stellar mass in any given galaxy, and this could be a very powerful tool. We now investigate the affect of galaxy size on the overall star formation rate.

Before going any further, one factor should be taken into account when interpreting the results of this analysis. The psf of IRAS was not capable of resolving most nearby external galaxies, and this is certainly the case for this sample. In such an analysis, we are really only interested in the star formation in the disks of spiral galaxies. However, the use of IRAS fluxes means that the star formation rates presented in this letter may be contaminated by bulge and/or nuclear star formation. Furthermore, we have used the to-

tal 2MASS K magnitude, which will also have a significant bulge contribution. One may expect these two affects to cancel to some degree, although one should also consider that the bulge contribution to the K-band light is probably more significant than the bulge contribution to the far-infrared light. However, since the correlation in Fig. 1 is good, one can only assume that this affect is small for the current sample. It should be noted that any object with known nuclear activity was excluded from the sample.

Using equation 5 we have calculated the star formation rates in these galaxies. These are listed in Table 1. Since we have measurements of D_{25} for all of these galaxies, which

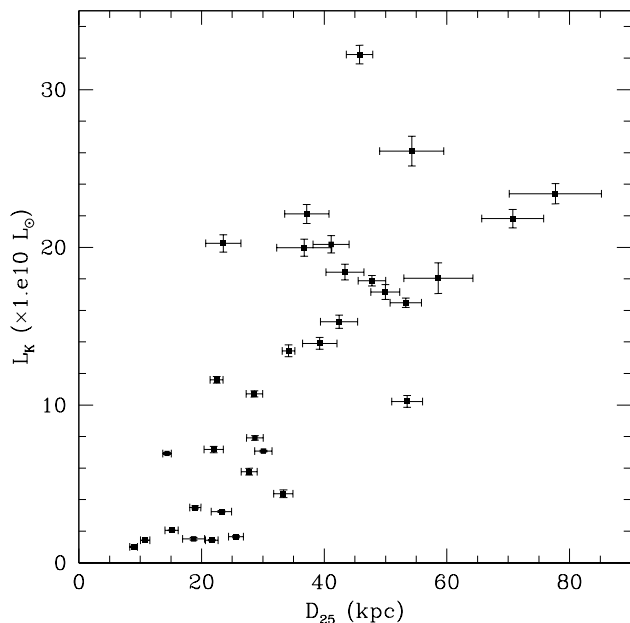


Figure 5. D_{25} diameter in kpc versus 2MASS K_s band luminosity.

have been taken from de Vaucouleurs et al. (1991), it is possible to measure the star formation rate per unit surface area, or the far-infrared luminosity per unit area, if we assume perfectly circular disks. One might expect that larger galaxies will also be more massive, at least in terms of their stellar mass. As a result, one might expect to see a correlation between shear rate and the far-infrared luminosity per unit area. Fig. 4 shows a plot of shear rate versus the far-infrared luminosity per unit area. Only a very weak, insignificant correlation is shown (correlation coefficient=0.13; significance=47.37 per cent). As a result, we decided to investigate the relationship between size, parameterized as D_{25} and K-band luminosity (or stellar mass) in disk galaxies, and this is shown in Fig. 5. There seems to be a weak, yet significant, correlation between these two parameters (correlation coefficient=0.35; significance=99.50 per cent). As a result it seems that while K band luminosity is a good means for estimating stellar mass (e.g. Brinchmann & Ellis 2000), it is not so good for the overall size of galaxies. Larger galaxies are not necessarily brighter in the near-infrared. However, on the average, galaxy size and mass do correlate, but for specific cases, it may not be possible to estimate either mass from size or size from mass. Also, the lack of a correlation in Fig. 4 may be a result of the weak correlation shown in Fig. 5.

From Fig. 1, it can be seen that there is a shear rate at which the star formation in disk galaxies switching off. In fact, from equation 4, this *critical* shear rate is $(\frac{\Delta}{\omega})_c = 0.70 \pm 0.09$. Using the correlation between shear rate and spiral arm pitch angle (Seigar et al. 2005), it can be shown that this critical shear rate would result in spiral structure with a pitch angle, $P_K = 10^\circ 6 \pm 2^\circ 5$, which is consistent with the tightest spiral structure typically seen in the near-infrared (e.g. Block et al. 1999). This also suggests that there would be a central mass concentration for which spiral galaxy disks are stabilised against gravitational collapse and subsequent star formation. One would expect that this critical shear

rate corresponds to the regime, where the Toomre stability parameter, $Q = 1$. This result implies that the correlation shown in Fig. 1 does contain some star formation physics, as it seems to accurately predict the tightest wound spiral arms observed in disk galaxies.

ACKNOWLEDGMENTS

This research has made use of the NASA/IPAC Extragalactic Database (NED) which is operated by the Jet Propulsion Laboratory, California Institute of Technology, under contract with the National Aeronautics and Space Administration. This publication makes use of data products from the Two Micron All Sky Survey, which is a joint project of the University of Massachusetts and the Infrared Processing and Analysis Center/California Institute of Technology, funded by the National Aeronautics and Space Administration and the National Science Foundation. The author wishes to thank the referee for useful suggestions which improved the content of this article.

REFERENCES

- Bertin G., 1991, in *Dynamics of Galaxies and Their Molecular Cloud Distributions*, Eds F. Combes and F. Casoli, IAU Symp. 146, Kluwer, Dordrecht, p93
- Bertin G., Lin C. C., 1996, *Spiral Structure in Galaxies: A Density Wave Theory*, MIT Press, Cambridge MA
- Block D. L., Stockton G., Grosbol P., Moorwood A. F. M., Peletier R. F., 1994, A&A, 288, 365
- Block D. L., Puerari I., Frogel J. A., Eskridge P. B., Stockton A., Fuchs B., 1999, Ap&SS, 269, 5
- Brinchmann J., Ellis R. S., 2000, ApJ, 536, L77
- Buat V., Xu C., 1996, A&A, 306, 61
- Burstein D., Rubin V. C., 1985, ApJ, 297, 423
- de Vaucouleurs G., de Vaucouleurs A., Corwin H. G., Jr, Buta R. J., Paturel G., Fouqué P., 1991, *The Third Reference Catalogue of Bright Galaxies*. Univ. Texas Press, Austin [RC3]
- Gavazzi G., Boselli A., Pedotti P., Gallazzi A., Carrasco L., 2002, A&A, 396, 449
- James P. A., et al., 2004, A&A, 414, 23
- Jeans J. H., 1929, *Astronomy and Cosmogony*, 2nd edition, Cambridge, England, Cambridge University Press
- Lonsdale C. J., Helou G., Good J. C. Rice, W. L., 1985, *Cataloged galaxies and quasars observed in the IRAS survey*, Pasadena: Jet Propulsion Laboratory
- Rubin V. C., Ford W. K. Jr., Thonnard N., 1980, ApJ, 238, 471
- Rubin V. C., Ford W. K. Jr., Thonnard N., Burstein D., 1982, ApJ, 261, 439
- Rubin V. C., Burstein D., Ford W. K. Jr., Thonnard N., 1985, ApJ, 289, 81
- Seigar M. S., James P. A., 1998a, MNRAS, 299, 685
- Seigar M. S., James P. A., 1998b, MNRAS, 299, 672
- Seigar M. S., Block D. L., Puerari I., 2004, in *Penetrating Bars Through Masks of Cosmic Dust: The Hubble Tuning Fork Strikes A New Note*, eds D. L. Block, I. Puerari, D. Ferreira, E. Block, Kluwer, Dordrecht, p 155

Seigar M. S., Block D. L., Puerari I., Chorney N. E., James P.A., 2005, MNRAS, in press [astro-ph/0502587]

Spinoglio L., Malkan M. A., Rush B., Carrasco L., Recillas-Cruz E., 1995, ApJ, 453, 616

Toomre A., 1964, ApJ, 139, 1217